Int J Clin Exp Pathol 2016;9(4):4203-4211
www.ijcep.com /ISSN:1936-2625/IJCEP0020651

Original Article

Morphological changes of the trabecular bone in osteonecrosis of the femoral head

Fan Yang*, Zhen-Zhong Zhu*, Shi-Yang Weng*, You-Shui Gao, Yang Wang, Jia-Gen Sheng, Chang-Qing Zhang

Department of Orthopedics, Sixth People's Hospital Affiliated to Shanghai Jiao Tong University, Shanghai, China.
**Equal contributors.*

Received November 27, 2015; Accepted January 26, 2016; Epub April 1, 2016; Published April 15, 2016

Abstract: This study compared the differences between the three-dimensional structure of normal trabecular bone and osteonecrosis necrosis of the femoral head (ONFH) from different causes. Specimens from 12 patients with ONFH were collected after total hip arthroplasty (Ficat II) and six specimens were collected from a group with fractures of the femoral neck. Micro-computer tomography (micro-CT) scans were performed on all specimens and the morphological parameters of different regions of the trabecular bone were measured. The patients were divided into the following three groups: idiopathic group, corticosteroids group and fracture group. In the fracture group, the trabecular bone volume fraction (BV/TV) and structure model index (SMI) were significantly higher than that of the other two groups ($P < 0.05$). The results among groups in various regions of the bone showed that the BV/TV in idiopathic group and corticosteroids group was below that in the fracture group. Meanwhile, the trabecular bone spacing in the first two groups was higher than that in the fracture group. Within each group, the morphology of the trabecular bone in the idiopathic group and corticosteroids group substantially changed according to the different region of the bone. Our studies demonstrated that ONFH results in structural disorders of the trabecula and loss of bone mass, especially in the corticosteroids group. The trabecular bone structure under the cartilage is remarkably different in different regions of the bone. Between the necrosis and repair areas, a large difference in trabecular morphology might be the key to fractures and collapse.

Keywords: Osteonecrosis of the femoral head, Micro-CT, pathologic morphology

Introduction

Osteonecrosis of the femoral head (ONFH) is a disease that is characterized by the death of bone trabecula and marrow in the femoral head. The disease is considered severe because it always leads hip arthroplasty [1, 2]. Approximately 5.0~12% of the all hip replacements were necessary because of this disease [3, 4]. Because necrotic bone is absorbed and new bone is formed, there tends to be poor mechanical support, which induces the collapse of the femoral head [5-7].

There are several studies on ONFH and core decompression is one process by which damage from the disease can be repaired. According to this process, the pathology of avascular necrosis of femoral head can be divided into the following five areas: articular cartilage zone, central zone of necrosis, fibrous tissue, sclerotic, and healthy [8]. The relationship between restoration of the femoral head and a decrease in mechanical strength is uncertain, but it is known that a reduction in mechanical strength as well as the continuous mechanical load leads to the final collapse of the femoral head; therefore, it is necessary to investigate the changes in bone trabeculae in different regions to explore the mechanism of femoral head collapse.

This study investigated the correlations between bone volume fraction and morphometric parameters in both ONFH and femoral neck fractures. In the ONFH group, the morphological changes from were investigated according to two main parameters: idiopathic and corticosteroid use. The fracture group was used as the normal control.

The aim in this study was to propose an approach for comparing the structure of the trabecula among the idiopathic group, corticoste-

Table 1. Characteristics of patients and controls

Variables	Idiopathic group	Corticosteroids group	Fracture group	P
Patients/hips (n)	6/6	6/6	6/6	
Age (years)	55 (48~62)	55 (43~66)	61 (56~64)	0.33
Male/female (patients)	5/1	5/1	5/1	1.00
Right/left (hips)	2/4	2/4	2/4	
Ficat-Arlet stage	stage II	stage II	stage II	
The distance from subchondral bone to fiber repair area (mm)*	1.35±0.1378	1.0333±0.1862	---	< 0.05

No statistically significant differences between the groups of patients' age. Based on the differences in age and sex among the groups, all the osteonecrosis cases were classified as Ficat stage II and were confirmed by postoperative pathologic findings of ONFH. *Values are means ± standard deviation.

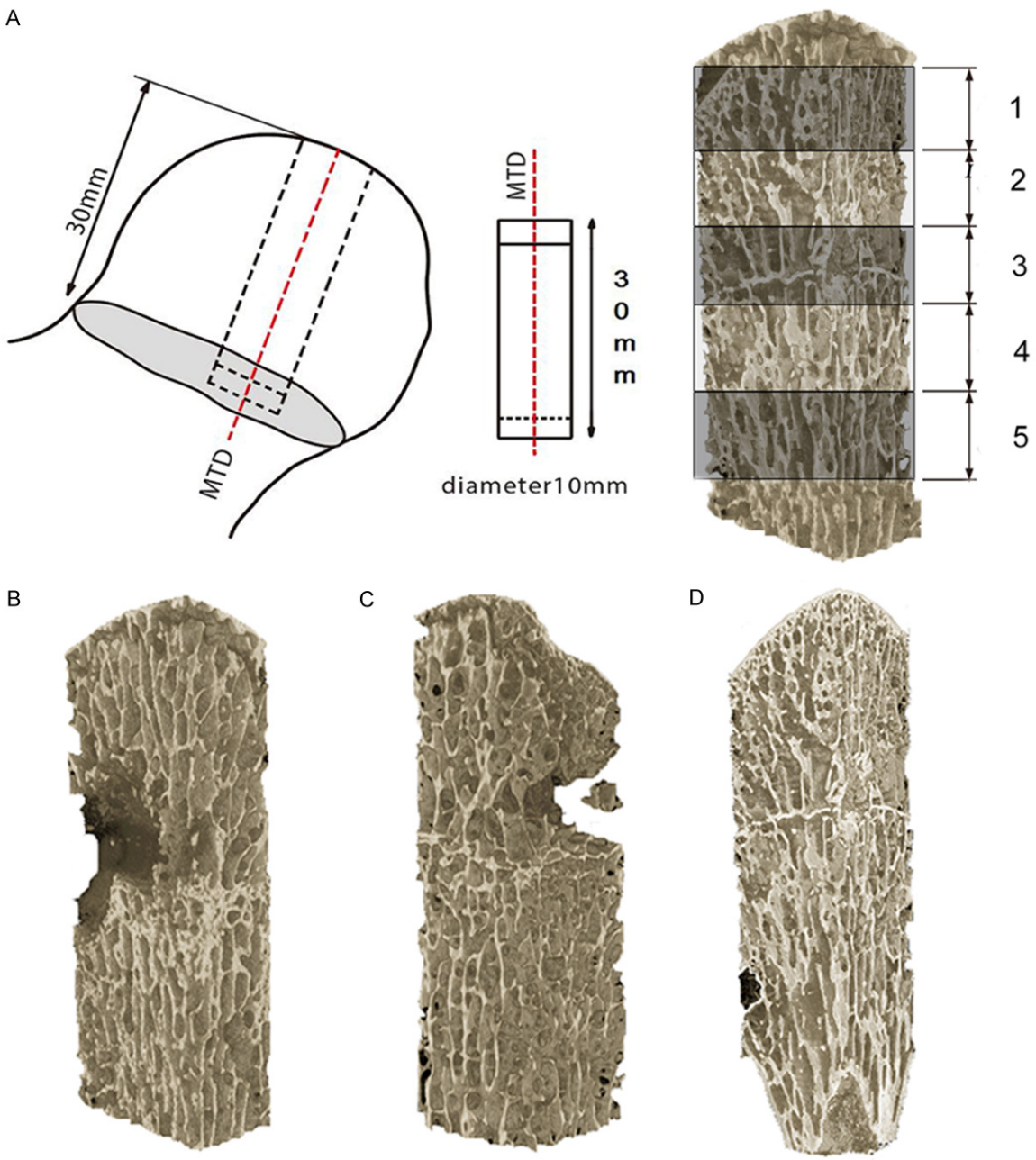

Figure 1. Typical examples of 3D reconstructed models. A. Extracting samples from the femoral head along the main trabecular direction (MTD); cuboids of bone (30×10×10 mm) were created for each cross section, and were divided into 5 sections. B. Bone sample from the idiopathic group. C. Bone sample from the corticosteroids group. D. Bone sample from the fracture group. The structure of the trabecula bone in the fracture group is more normal than that in the other two groups.

roids group and fracture group, and exploring the tendency toward continuous variation in the subchondral trabeculae in each group.

Materials and methods

Donor selection and bone specimen preparation

Specimens of femoral heads were collected from three clinical groups-idiopathic group, corticosteroids group and fracture group (**Table 1**). The specimens from all groups were obtained from patients who underwent artificial hip replacement between December 2011 and February 2014. All specimens were stored at -80°C until analyzed.

All the thawed femoral heads were stored in a 70% ethanol solution for at least 4.0 weeks. To better reflect the morphological changes in the trabecula necrosis area, all samples were extracted along the main trabecular direction (MTD), which was identified by X-ray of the femoral head before extraction. First, the specimen was cut into 10-mm thick hemisphere bone pieces along the central coronal plane of the femoral head. Then, the hemisphere bone was cut into 10-mm-wide slices parallel to MTD, and MTD was used as central line. Finally, a 30×10×10 mm^3 bone slice was obtained (**Figure 1A**).

Micro-CT scanning

All samples were scanned using a Skyscan 1,176 m CT scanner (Bruker microCT N.V., Luxemburg, Belgium). The micro-CT scans were done with a complete rotation over 185°, 90 kVp tube voltage, and 270 μA tube current, using a 0.1-mm-thick Cu filter to reduce beam hardening a 20- by 20-mm field of view, and 17.93-μm isotropic pixel size. The bone specimen was scanned to 20 mm in its free height starting from the bone-end cap interface. After acquiring the image, a stack of 1,674 cross sections were reconstructed (1024×1024 pixels each), with an interslice distance of 1.0 pixel, corresponding to a total height of 20 mm. The reconstruction was done using a filtered back-projection algorithm and Cone_rec (Skyscan, Belgium) [9] and storing each cross section as a 16-bit image (256 grey levels). To calculate the structural parameters, the cross sections were binarized using a uniform threshold and 3D-Calculator (Skyscan), with the threshold level set according to a previously published protocol [10]. For each cross section, a square region of interest (ROI) was delineated and centered on the bone specimen containing only cancellous bone. To avoid the inclusion of debris from cutting the bone, each ROI was 8.0 mm long and an external annulus 0.2 mm thick was excluded. For each specimen, the following structural 3D parameters were determined over the chosen volume of interest (VOI): the bone volume fraction (BV/TV), trabecular thickness (Tb.Th), trabecular number (Tb.N), trabecular separation (Tb.Sp), and structure model index (SMI). SMI [11]. Evaluates the type of structure for each sample. An ideal plate model has an SMI of 0, whereas an ideal cylindrical rod has an SMI of 3. The degree of anisotrophy (DA), the ratio of the longest length divided by the shortest H vector, was used to define the structural orientation. An isotropic structure has a DA of 1, whereas an anisotropic structure has a DA value > 1. In this study, each specimen was assessed using two different approaches-global analysis and local analysis.

The global analysis consisted of calculating all parameters over the entire specimen volume. VOI was composed of a stack of 1,674 consecutive ROIs, resulting in a cuboid VOI 8.0 mm wide, 8.0 mm high, and 30 mm long.

A local analysis was computed along the entire specimen height using a sliding VOI of 3.5 mm (i.e., 196 consecutive ROIs) high. This height was set to satisfy the continuum assumption for analysis of the trabecula, which specifies that the minimum dimension must be greater than five trabecular spacings [12]. The trabecular spacing of the human femoral head tissue is ~0.7 mm [13]. Therefore, 3.5 mm was chosen as the height to use. (**Figure 1A**) Five sections

Table 2. Difference in structural parameters among the groups from the global analysis assessed using microcomputed tomography (17.93 μm)

	Idiopathic group	Corticosteroids group	Fracture group	P
BV/TV (%)	36.46±4.71	35±5.36	43.41±3.99	< 0.05**,#
SMI	0.16±0.57	-0.3±0.74	1.51±0.81	< 0.05**,#
Tb.Th (mm)	0.32±0.05	0.36±0.08	0.38±0.02	0.139
Tb.N (1/mm)	1.15±0.13	1±0.15	1.14±0.09	0.089*
Tb.Sp (mm)	0.69±0.06	0.88±0.23	0.58±0.10	< 0.05*,**,#
DA	9.43±9.68	11.89±7.5	25.09±28.96	0.304

Fracture samples showed a significant increase in BV/TV, SMI ($P < 0.05$), and DA ($P = 0.304$) and a significant decrease in Tb.Sp ($P < 0.05$). The corticosteroids group had a lower Tb.N ($P < 0.05$) and a higher Tb.Sp ($P = 0.139$) than the idiopathic group. Values are means ± standard deviation. Significant differences are indicated as: *idiopathic group versus corticosteroids group; **idiopathic group versus fracture group; #corticosteroids group versus fracture group.

were created and numbered from 1 to 5. The first two sections were from the subchondral bone and based on the pathological sections; the last three sections were from the top of the fiber repair area.

Histopathological examinations

All specimens were embedded in methyl methacrylate according to a routine laboratory procedure. Five micrometer sections of specimens were stained with Masson's trichrome. The distance was calculated from the subchondral bone to the fiber repair area from the ONFH group and the mean distance of this area in the two groups was used to determine the beginning of the third segment in all groups (**Table 1**). The last two sections were a continuation of the third section.

Statistical analyses

Variables were tested for normality of distribution using the Shapiro-Wilk test and natural logarithm transformation was applied when necessary. The differences among the three groups in age and sex were assessed using one-way analysis of variance and a Sidak post hoc method. The least significant difference was used to assess the differences within each group. SAS version 9.3 (SAS Institute, Inc., Cary, NC, USA) was used and $P < 0.05$ was considered statistically significant. Based on local analysis, a line chart on each variable was also constructed. All values are reported as the mean ± standard error.

Results

As shown in **Table 1**. No statistically significant differences between the groups of patient's age. Based on the differences in age and sex among the groups, these variables were used as covariates in the statistical analyses and the results are presented as age and sex, respectively. According to a simple radiograph, all the osteonecrosis cases were classified as Ficat stage II and were confirmed by postoperative pathologic findings of ONFH. For patients in the idiopathic ONFH group, no identifiable risk factors, for example, alcohol and tobacco, were associated with the disease; For patients in ONFHs group, patients with trauma factors, such as fracture of femoral neck were not included in the study.

Micro-CT scanning

Typical examples of 3D reconstructed models are shown in **Figure 1**. Large cavities under the subchondral bone were identified in the ONFH group. The structure of trabecular bone in the idiopathic and corticosteroid groups was more irregular than that in the control group. In all experimental samples, a strip of trabecular bone was found parallel to the tangent of cartilage surface. A 3D micro-CT representation of global analysis is reported in **Table 2**. Fracture samples showed a significant increase in BV/TV, SMI ($P < 0.05$), and DA ($P = 0.304$) and a significant decrease in Tb.Sp ($P < 0.05$). The corticosteroids group had a lower Tb.N ($P < 0.05$) and a higher Tb.Sp ($P = 0.139$) than the idiopathic group.

In local analysis (**Figure 2**), regardless of subsection, BV/TV and SMI in the fracture group was significantly increased; the opposite was true of Tb.Sp. BV/TV in the idiopathic group was much higher than that in the corticosteroids group in section 4 ($P < 0.05$), and compared with sections 1, 4, and 5 in the fracture group, the Tb.SB in the corticosteroids group was significantly increased ($P < 0.05$).

The line chart of each section in the three groups is shown in **Figure 3**. The variation trend

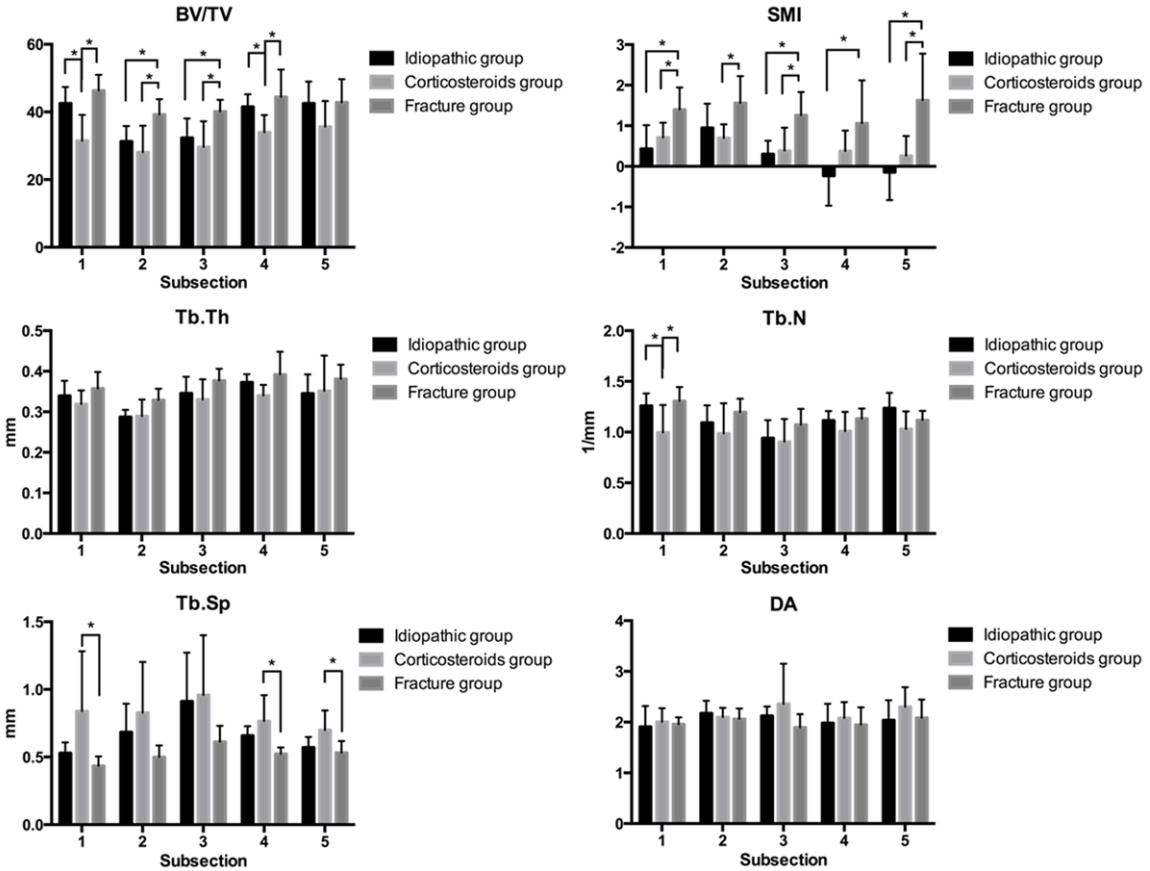

Figure 2. Significant differences in bone among the groups. BV/TV and SMI in the fracture group was significantly increased; the opposite was true of Tb.Sp. BV/TV in the idiopathic group was much higher than that in the corticosteroids group in section 4, and compared with sections 1, 4, and 5 in the fracture group, the Tb.SB in the corticosteroids group was significantly increased (*P < 0.05).

in each section in the fracture group is more placid. In all groups, BV/TV, Tb.Th, and Tb.N showed significant decreases between sections 1 and 2 and increases from sections 3 to 5. Compared with the idiopathic and corticosteroids groups, the fracture group maintained a higher trend in these parameters. The changes in SMI in the idiopathic group were more intense. All groups showed a high point of Tb.Sp in section 3.

Histological analysis

In our specimens, the microscopic aspects varied with each patient and there might have been different findings in the same patient, which is dependent on the area of the femoral head that was studied. Inside the area of necrosis (sections 1 and 2), the trabecula bones were significantly narrowed without integrity. In all patients, including those in the ONFH group, an extensive area of fibrous tissue was found in which nearly all bone tissues were perpendicular to MTD (section 3). In the remote areas of articular cartilage (sections 4 and 5), osteoblasts were arranged in the shape of bone trabeculae and osteoids were formed (**Figure 4**).

Discussion

In this study, bones from the femoral head of patients with femoral neck fracture or ONFH were compared and analyzed. ONFH is an illness with a controversial etiology, the trigger of which is supposed to be the suppression to the blood flow to the femoral head [14]. Multiple theories have attempted to explain the pathogenesis of ONFH; however, the causes and mechanisms are still unknown. Thus, to diagnose the disease at an early stage, physicians must be able to identify their patients' risk factors. The main known risk factors are trauma, smoking, corticosteroid therapy, and chronic alcohol consumption. The relative frequency of

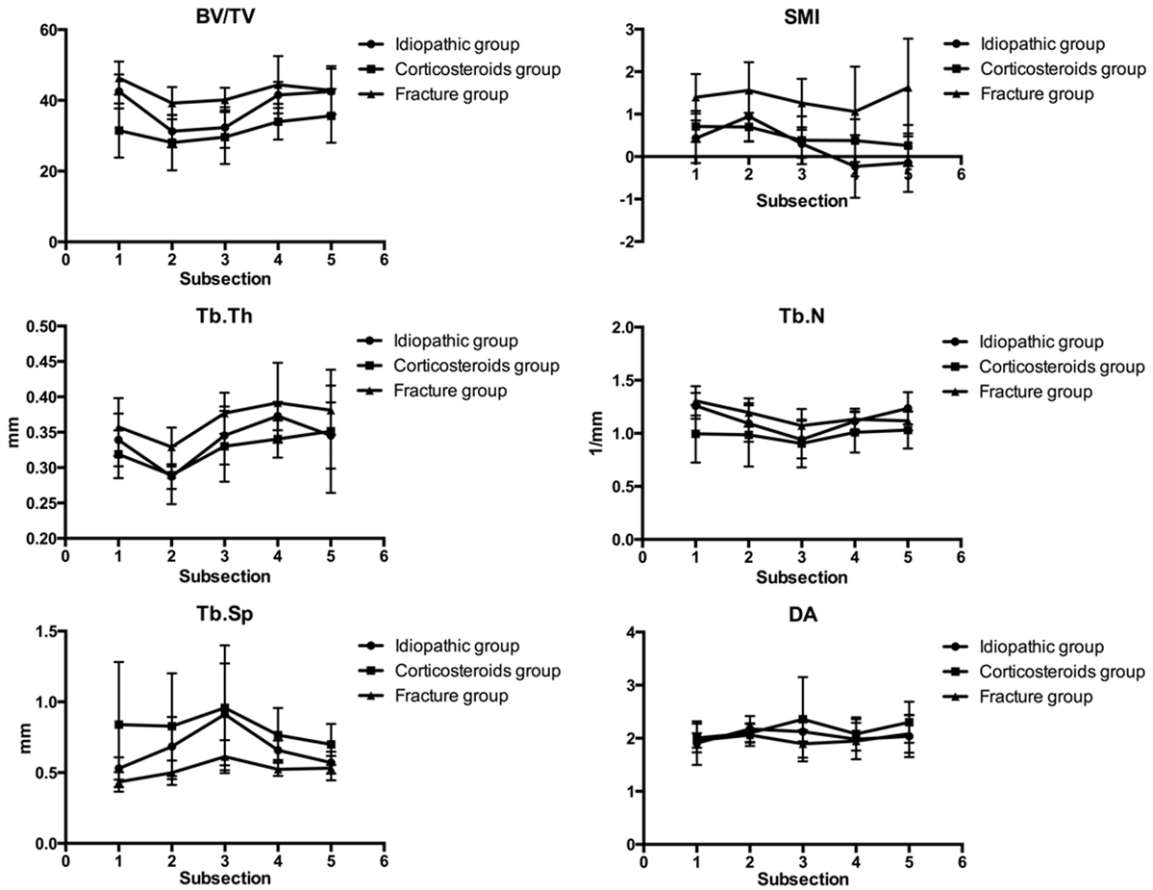

Figure 3. Line chart of each section in the different groups. The variation trend in each section in the fracture group is more placid. In all groups, BV/TV, Tb.Th, and Tb.N showed significantly decreased from sections 1 to 2, and increased from sections 3 to 5.

the most common causes of ONFH are alcoholism, 20-40%, and corticosteroid therapy, 35-40%; the remaining are idiopathic (20-40%) [15, 16]. Most studies were limited by the lack of a comparison among different etiologies, normal control groups, and research done before the collapse of the femoral head [17]. Ficat stage I hips have normal, plain radiographs and dead bone appears similar to live bone. In this paper, all osteonecrosis cases were Ficat stage II, in which the secondary repair process with the formation of new bone on top of dead trabeculae appears and dystrophic calcification of the marrow can be found on plain film. The typical stage II lesion is a mottled radiodensity with a preserved articular contour [18].

Eighteen patients were included in this study. In the ONFH group, the loss of trabecula bone structure was found to be caused by a subchondral fracture and repaired after ONFH. In all specimens, there was one layer of trabecula bone perpendicular to MTD. It is unknown whether this was a closure of the epiphysis line. Based on the global analysis, the ONFH group showed significant decreases in BV/TV and significant increases in Tb.Sp compared to the fracture group; these figures indicated loss of bone mass. The characteristics of the study groups are summarized in **Figure 3**. BV/TV was significantly increased in the fracture group while Tb.Sp decreased, and the corticosteroids group lost more bone mass than either the idiopathic or fracture group. These results were in accordance with Darrell et al. [19]. Increased cortical hormone levels in the body have been identified as having a direct inhibitory effect on the function of osteoblasts, which will, in turn, depress the formation of bone. In addition, the bone blood vessels are directly damaged. High levels of cortical hormones also have an enhancing effect on osteoclast function. Thus, bone brittleness increases and bone growth decreases. All of these factors aggravate osteo-

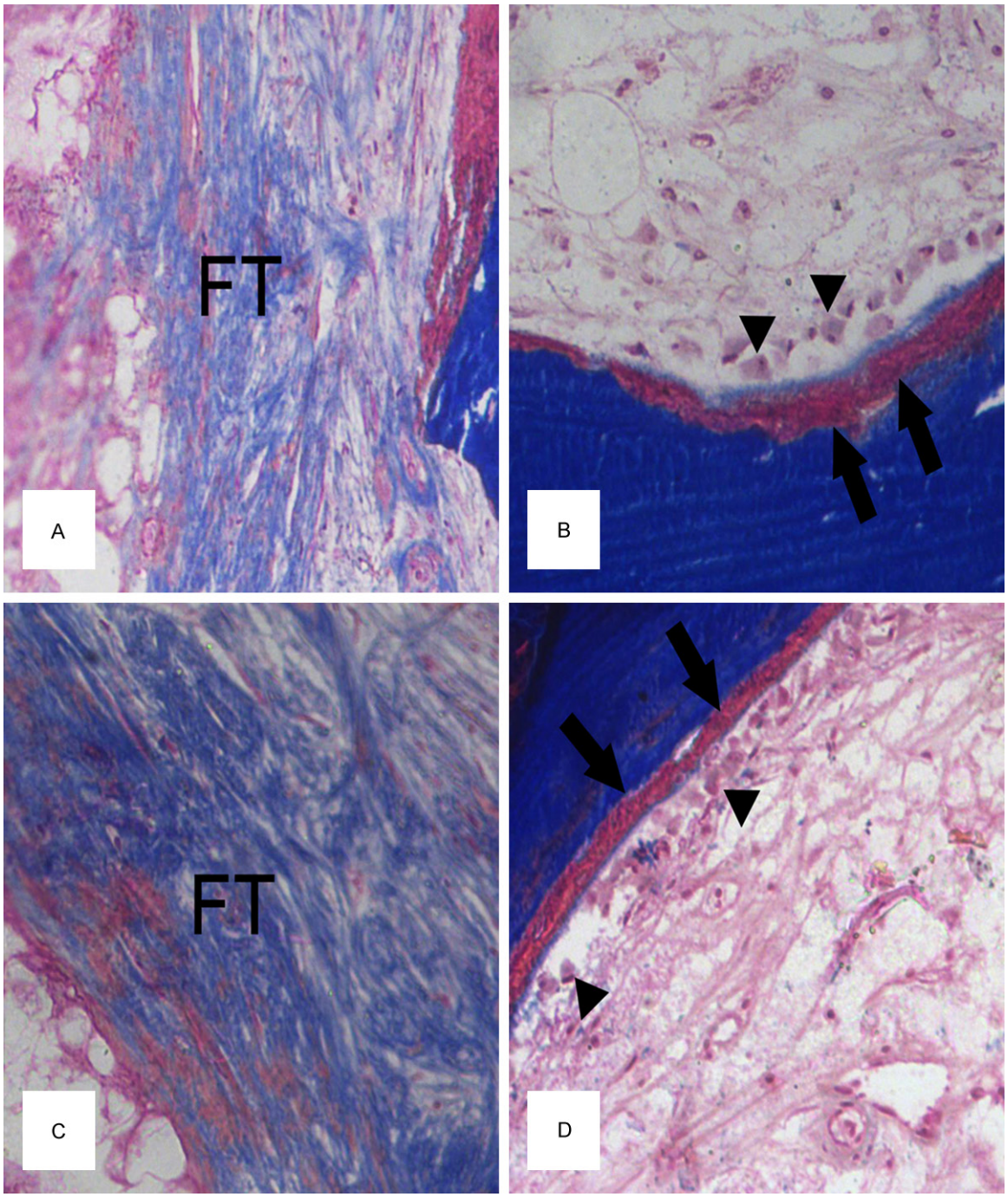

Figure 4. Histological features in both areas of fibrous tissue and the formation of osteoids. A, B. Idiopathic group; C, D. Corticosteroids group; FT: fiber repair area showing areas of fibrous tissue. The formation of osteoids (thick arrows) and osteoblasts arranged in the shape of trabeculae (thin arrows). All images: hematoxylin-eosin and trichrome staining; scale bars 150 μm.

porosis and inhibit the formation of the neoformative bones.

It is found that the morphology of trabecula bone changes greatly between the articular cartilage and fibrous repair area. The ONFH group had a significant loss of bone mass and bone trabecula structure disorder under the cartilage compared to that in the fracture group. The idiopathic group had more dramatic trends in change; the changes in trabecular bone morphological were quite obvious between sections 3 and 4 compared to that of the corticosteroids group. There might be osteopo-

rosis in the corticosteroids group [20], in which changes of the trabecula bone were not obvious. These differences indicated that the corticosteroids group had a worse modulus of elasticity, and fracture in this junction area will easily occur according to this result. In addition, the DA of the corticosteroids group was higher than that in the fracture group. It is ascribed that similar DA is considered to be important in sustaining normal bone remodeling for load bearing [21]. Our studies revealed that the mechanical transmission on the bone in the corticosteroids group was damaged. Min et al. [22]. Reviewed 10 patients with ONFH induced by a femur neck fracture that occurred in the zone between the necrotic region and the reparative interface and extended downward through it. This could be explained by a previous 3D finite-element model study [23]. That showed that high stress was applied in the deep necrosis area where the necrotic-viable bone interfaced with a large necrotic lesion. It can be observed from the line chart that the necrotic area encompasses no more than section 5. This might reveal the extent of necrosis along MTD in Ficat stage II.

Conclusion

After ONFH, there are necrotic trabecula bone structure disorders and loss of bone mass. Compared with the idiopathic and fracture groups, the corticosteroids group had a lower bone mass and less of a change in each section. Between the necrotic and repair areas, the greater difference in trabecular morphology might be the key to fractures and collapse. Further research with more samples is needed to support these results.

Acknowledgements

This research was supported by the Shanghai Municipal Science and Technology Commission Medical Key Project (11411950400) and Shanghai Municipal Hospital New Technology Joint Research Project (SHDC12012115).

Disclosure of conflict of interest

None.

Address correspondence to: Chang-Qing Zhang and Jia-Gen Sheng, Sixth People's Hospital Affiliated to Shanghai Jiao Tong University, Shanghai Jiao Tong University, 600 Yishan Road, Shanghai 200233, China. Tel: +86-21-64369181; Fax: +86-21-6470-1361; E-mail: zhangcq@sjtu.edu.cn (CQZ); shengjiagen@126.com (JGS)

References

[1] Mont MA, Marulanda GA, Jones LC, Saleh KJ, Gordon N, Hungerford DS, Steinberg ME. Systematic analysis of classification systems for osteonecrosis of the femoral head. J Bone Joint Surg Am 2006; 88 Suppl 3: 16-26.

[2] Gagala J, Buraczynska M, Mazurkiewicz T, Ksiazek A. Prevalence of genetic risk factors related with thrombophilia and hypofibrinolysis in patients with osteonecrosis of the femoral head in Poland. BMC Musculoskelet Disord 2013; 14: 264.

[3] Steinberg ME, Hayken GD, Steinberg DR. A quantitative system for staging avascular necrosis. J Bone Joint Surg Br 1995; 77: 34-41.

[4] Lavernia CJ, Sierra RJ, Grieco FR. Osteonecrosis of the femoral head. J Am Acad Orthop Surg 1999; 7: 250-61.

[5] Pringle D, Koob TJ, Kim HK. Indentation properties of growing femoral head following ischemic necrosis. J Orthop Res 2004; 22: 122-30.

[6] Ha YC, Kim HJ, Kim SY, Kim KC, Lee YK, Koo KH. Effects of age and body mass index on the results of transtrochanteric rotational osteotomy for femoral head osteonecrosis. J Bone Joint Surg Am 2010; 92: 314-21.

[7] Kim HK, Su PH. Development of flattening and apparent fragmentation following ischemic necrosis of the capital femoral epiphysis in a piglet model. J Bone Joint Surg Am 2002; 84-A: 1329-34.

[8] Arlet J, Ficat C. Ischemic necrosis of the femoral head. Treatment by core decompression. J Bone Joint Surg Am 1990; 72: 151-2.

[9] Sasov A, Van Dyck D. Desktop X-ray microscopy and microtomography. J Microsc 1998; 191: 151-8.

[10] Perilli E, Baruffaldi F, Visentin M, Bordini B, Traina F, Cappello A, Viceconti M. MicroCT examination of human bone specimens: effects of polymethylmethacrylate embedding on structural parameters. J Microsc 2007; 225: 192-200.

[11] Hildebrand T, Ruegsegger P. Quantification of Bone Microarchitecture with the Structure Model Index. Comput Methods Biomech Biomed Engin 1997; 1: 15-23.

[12] Harrigan TP, Jasty M, Mann RW, Harris WH. Limitations of the continuum assumption in cancellous bone. J Biomech 1988; 21: 269-75.

[13] Ulrich D, van Rietbergen B, Laib A, Ruegsegger P. The ability of three-dimensional structural

indices to reflect mechanical aspects of trabecular bone. Bone 1999; 25: 55-60.
[14] Taylor D, Hazenberg JG, Lee TC. Living with cracks: damage and repair in human bone. Nat Mater 2007; 6: 263-8.
[15] Mont MA, Hungerford DS. Non-traumatic avascular necrosis of the femoral head. J Bone Joint Surg Am 1995; 77: 459-74.
[16] Jones LC, Hungerford DS. Osteonecrosis: etiology, diagnosis, and treatment. Curr Opin Rheumatol 2004; 16: 443-9.
[17] Chernetsky SG, Mont MA, LaPorte DM, Jones LC, Hungerford DS, McCarthy EF. Pathologic features in steroid and nonsteroid associated osteonecrosis. Clin Orthop Relat Res 1999; 149-61.
[18] Feldkamp LA, Goldstein SA, Parfitt AM, Jesion G, Kleerekoper M. The direct examination of three-dimensional bone architecture in vitro by computed tomography. J Bone Miner Res 1989; 4: 3-11.
[19] Fisher DE, Bickel WH. Corticost eroid-induced avascular necrosis. J Bone Joint Surg Am 1971; 53: 859.
[20] Wang GJ, Sweet DE, Reger SI, Thompson RC. Fat-cell changes as a mechanism of avascular necrosis of the femoral head in cortisone-treated rabbits. J Bone Joint Surg Am 1977; 59: 729-35.
[21] Ding M, Odgaard A, Linde F, Hvid I. Age-related variations in the microstructure of human tibial cancellous bone. J Orthop Res 2002; 20: 615-21.
[22] Min BW, Koo KH, Song HR, Cho SH, Kim SY, Kim YM, Kang CS. Subcapital fractures associated with extensive osteonecrosis of the femoral head. Clin Orthop Relat Res 2001; 227-31.
[23] Yang JW, Koo KH, Lee MC, Yang P, Noh MD, Kim SY, Kim KI, Ha YC, Joun MS. Mechanics of femoral head osteonecrosis using three-dimensional finite element method. Arch Orthop Trauma Surg 2002; 122: 88-92.